Raman and Infrared Reflectivity Determination of Phonon Modes and Crystal Structure of Czochralski-Grown $NaLnF_4$ (Ln = La, Ce, Pr, Sm, Eu, and Gd) Single Crystals

Márcio M. Lage,[†] Roberto L. Moreira,*[,†] Franklin M. Matinaga,[†] and Jean-Yves Gesland[‡]

Departamento de Física, ICEx, UFMG, C.P. 702, 30123-970 Belo Horizonte (MG), Brazil, and Université du Maine-Cristallogénèse, UMR 6087, 72085 Le Mans Cedex 9, France

Received April 22, 2005. Revised Manuscript Received June 21, 2005

Optical quality $NaLnF_4$ single crystals have been obtained from nonstoichiometric melts through the Czochralski technique, for Ln = La, Ce, Pr, Sm, Eu, and Gd. These crystals are potential laser host materials because of their high luminescence efficiency when doped with rare earth ions. In view of this application, the knowledge of the optical phonon modes of the crystals is mandatory. In this work, we present our polarized Raman scattering and infrared reflectivity studies of $NaLnF_4$ single crystals for large ionic radius lanthanides. For the different Ln ions, the spectra in each polarized configuration appeared to be very similar; the effect of Ln ion substitution on the crystal's vibrational modes was generally the hardening of the modes with decreasing ionic radii, with no important symmetry evolution. For all investigated crystals, the symmetries and number of observed phonon modes agree well with group theory predictions for the hexagonal $P\bar{6}$ group. The rather broad phonon bands and the presence of defect modes evidence the cationic disorder allowed by this structure.

1. Introduction

Rare earth doped $NaLnF_4$ (Ln = lanthanide ion) and $NaYF_4$ crystals exhibit high luminescence efficiency,[1−5] comparable to the classical $LiYF_4$ sheelite (YLF), one of the most used hosts for solid state lasers.[6] Hence, these materials have been suggested for such applications, since fluoride crystals also fulfill other important laser requirements, namely, low cutoff phonon frequencies, high resistance against short wavelength radiation, high optical damage threshold, and low nonlinear refractive indices.[2,4,6] Also worthy of mention is the fact that $NaYF_4$ appears to be the most efficient material for green and blue up-conversion.[4,7] However, the crystals available so far had sub-millimeter dimensions, owing to their incongruent melt,[8,9] while YLF-like crystals for current laser applications have centimeter sizes.[6] Recently, we have developed a technique to pull large (several cubic centimeters) optical quality $NaLnF_4$ single crystals from nonstoichiometric melt, by the Czochralski method, opening the possibility of studying the characteristic features of the optical phonon modes of these materials, in view of that application.[10] In particular, a study on $NaLaF_4$ showed that this crystal belongs to a piezoelectric group and that its polarized infrared and Raman base functions have symmetry properties compatible with the hexagonal $P\bar{6}$ structure.[10]

The determination of the crystal structure of $NaLnF_4$ and $NaYF_4$ crystals has been a matter of debate for more than 50 years. In fact, the structures proposed for those materials differ among different authors and for different lanthanide or yttrium ions. Zachariasen proposed the trigonal $P321$ group (D_3^2), for $NaLaF_4$ and $NaCeF_4$,[11] while Sobolev et al. proposed the hexagonal gagarinite structure, $P6_3/m$ (C_{6h}^2), for the $NaYF_4$ crystal.[12] The gagarinite structure was confirmed by Burns for $NaYF_4$, $NaSmF_4$, and $NaTmF_4$, who found, nonetheless, a different hexagonal structure $P\bar{6}$ (C_{3h}^1) for Ln = La−Nd, Eu−Tb, Ho, and Er, while his structural study on $NaDyF_4$ was inconclusive.[13] More recently, Fedorov et al. investigated several crystals (Ln = La−Nd, Sm, Tb, Dy, and Er−Lu) and described them as belonging to the gagarinite structure.[14−16] However, Zakaria et al.,[3] Grzechnik et al.,[17] and Mech et al.[5] refined their X-ray data on Eu-, Y-,

* Corresponding author. E-mail: bmoreira@fisica.ufmg.br.
[†] UFMG.
[‡] Université du Maine-Cristallogénèse.

(1) Kiliaan, H. S.; Kotte, J. F. A. K.; Blasse, G. *Chem. Phys. Lett.* **1987**, *133*, 425.
(2) Zakaria, D.; Fournier, M. T.; Mahiou, R.; Cousseins, J. C. *J. Alloys Compd.* **1992**, *188*, 250.
(3) Zakaria, D.; Mahiou, R.; Avignant, D.; Zahir, M. *J. Alloys Compd.* **1997**, *257*, 65.
(4) Martin, N.; Boutinaud, P.; Malinowski, M.; Mahiou, R.; Cousseins, J. C. *J. Alloys Compd.* **1998**, *275*, 304.
(5) Mech, A.; Karbowiak, M.; Kepinski, L.; Bednarkiewicz, A.; Strek, W. *J. Alloys Compd.* **2004**, *380*, 315 .
(6) Kaminskii, A. A. *Laser Crystals*; Springer: Berlin, 1990.
(7) Krämer, K. W.; Biner, D.; Frei, G.; Güdel, H. U.; Hehlen, M. P.; Lüthi, S. R. *Chem. Mater.* **2004**, *16*, 1244.
(8) Thoma, R. E.; Hebert, G. M.; Insley, H.; Weaver, C. F. *Inorg. Chem.* **1963**, *2*, 1005.
(9) Thoma, R. E.; Insley, H.; Hebert, G. M. *Inorg. Chem.* **1966**, *5*, 1222.
(10) Lage, M. M.; Matinaga, F. M.; Gesland, J.-Y.; Moreira, R. L. To be published.
(11) Zachariasen, W. H. *Acta Crystallogr.* **1948**, *1*, 265.
(12) Sobolev, B. P.; Mineev, D. A.; Pashutin, V. P. *Dokl. Akad. Nauk SSSR* **1963**, *150*, 791.
(13) Burns, J. H. *Inorg. Chem.* **1965**, *4*, 881.
(14) Fedorov, P. P.; Buchinskaya, I. I.; Bondareva, O. S.; Vistin, L. L.; Bystrova, A. A.; Sobolev, B. P. *Russ. J. Inorg. Chem.* **1996**, *41*, 1633.
(15) Fedorov, P. P.; Buchinskaya, I. I.; Bondareva, O. S.; Vistin, L. L.; Sobolev, B. P. *Russ. J. Inorg. Chem.* **1996**, *41*, 1823.
(16) Fedorov, P. P.; Buchinskaya, I. I.; Bondareva, O. S.; Bystrova, A. A.; Vistin, L. L.; Ershov, D. A.; Ivanov, S. P.; Stasyuk, V. A.; Sobolev, B. P. *Russ. J. Inorg. Chem.* **2000**, *45*, 949.

10.1021/cm050860k CCC: $30.25
Published on Web 07/21/2005

and Gd-based crystals, respectively, with the Burns $P\bar{6}$ structure (note that Burns did not propose this group for the $NaYF_4$ crystal). Finally, Krämer et al.[7] proposed the gagarinite structure for a slightly nonstoichiometric mixed $Na(75\%\ Y + 25\%\ Yb)F_4$ crystal.

The crystal structure determines uniquely the number and symmetries of the optical phonon modes of any material, which, in turn, are key features of laser hosts designing. In this way, Raman and infrared spectroscopies are very suitable techniques for solving these problems, that is, for determining the phonon modes at the Brillouin zone center and, consequently, for confirming or indirectly proposing the crystal structure. Thus, in this work, we performed a systematic investigation into the optical vibrational properties and the structure of Czochralski-grown $NaLnF_4$ single crystals (Ln = La, Ce, Pr, Sm, Eu, and Gd), by using polarized Raman scattering and infrared reflectivity measurements. Our results, together with group theory tools, helped us to solve the crystal structure of the materials, besides giving the behavior of the optical phonon modes for the different lanthanides.

2. Experimental Section

2.1. Crystal Growth. $NaYF_4$ and $NaLnF_4$ compounds present an incongruent melting point, as shown by the phase equilibrium diagrams of the $NaF-YF_3$ and $NaF-LnF_3$ systems, determined by Thoma et al.[8,9] and Fedorov et al.[14−16] To obtain $NaLnF_4$ crystals, we used NaF-rich melts, where the amount of excess NaF was calculated for each crystal, as a quantity able to depress the melting point of the mixture to a value below the decomposition crystal temperature, by partial NaF melting (see ref 9). This method is analogous to the procedure developed to obtain YF_3 crystals, which also melt incongruently.[18] However, we could only obtain single crystals for large Ln ions, from La to Gd. For the other Ln ions and Y, we always obtained phase segregation; for this reason, these crystals will not be studied here. Large (several cubic centimeters) and transparent $NaLnF_4$ single crystals were pulled from those melts at very low speed rates (0.1 mm/h) through the Czochralski technique, for Ln = La, Ce, Pr, Sm, Eu, and Gd. The first seeds were obtained through polygermination on a platinum wire and traditional necking. The La, Ce and Gd-based crystals are transparent, while crystals with Pr, Sm, and Eu present, respectively, green, citrine and light brown colors. Laue photographs of the crystals showed that the preferential growth direction was always close to the hexagonal axis. The crystals were oriented by X-ray procedures and cut in form of cubes with 3 mm size, where two orthogonal directions were parallel to the crystallographic *z* (hexagonal axis) and *x* axes (a natural in-plane axis). The third orthogonal axis, *y*, is perpendicular to *z* and *x* and does not represent a crystal axis. For the optical measurements, the faces of the crystal were polished with diamond pastes to an optical grade (down to 0.25 μm).

2.2. Infrared Spectroscopy. The infrared measurements were done in a BOMEM-DA8 Fourier transform infrared spectrometer, with a specular reflectance accessory (external incidence angle of 11.5°), under mechanical vacuum. In the mid-infrared region (500−4000 cm^{-1}) we used a silicon carbide (Globar) source, a Ge-coated KBr beam splitter, a ZnSe polarizer, and a liquid-N_2-cooled HgCdTe detector. In the far-infrared range (30−500 cm^{-1}), we used a Hg-arc source, a 6-μm coated Mylar hypersplitter, a polyethylene-grid polarizer, and a liquid-He-cooled Si bolometer. The spectral resolution was typically 3 cm^{-1}, and the statistics were improved by accumulating, at least, 64 scans each time.

Table 1. Ln^{3+} Ionic Radii (*r*) for CNs = 9 or 6 and the Unit Cell Parameters (*V*, Unit Cell Volume) Common to the Groups $P\bar{6}$ and $P6_3/m$[a]

	La^{3+}	Ce^{3+}	Pr^{3+}	Sm^{3+}	Eu^{3+}	Gd^{3+}
r (Å), CN = 9	1.216	1.196	1.179	1.132	1.120	1.107
r (Å), CN = 6	1.032	1.01	0.990	0.958	0.947	0.938
a (Å)	6.177	6.1408	6.1226	6.051	6.040	6.035
c (Å)	3.8270	3.776	3.7444	3.640	3.632	3.614
V (Å^3)	126.5	123.3	121.55	115.4	114.7	114.0
ref	16	16	16	9	3	5

[a] The ionic radii were taken from ref 21. For the Na^+ ion, *r* = 1.24 and 1.02 for CN = 9 and 6, respectively.

2.3. Raman Spectroscopy. Raman backscattering measurements were performed using a Jobin-Yvon T64000 spectrometer equipped with an Olympus microscope (objective 10×) and a liquid-N_2-cooled CCD detector. The exciting source was an Ar^+-ion laser, operating in the 514.5-nm line, with a typical 30-mW power. The spectral resolution was better than 2 cm^{-1}, and the accumulation times were typically 20 collections of 10 s. All the spectra were corrected by the Bose factor[19] and then fitted by a sum of Lorentzian lines. The scattering geometries for the spectra presented in the text and figures follow the Porto's notation $k_i(e_ie_s)k_s$, where *k* and *e* are the wavevector and polarization directions of the incident (i) and scattered (s) light beams.[20]

3. Results and Discussions

3.1. Crystalline Structure and Group Theory Predictions. Although the first structure proposed for $NaLaF_4$ and $NaCeF_4$ was *P*321, the controversy which subsisted in the last 40 years around the structure of several members of the $NaLnF_4$ family and around $NaYF_4$ concerned the $P6_3/m$ and $P\bar{6}$ groups. Then, in the following, we will consider only the recent refinements within these two groups. In both cases, the crystalline formula should be written $Na_{1.5}Ln_{1.5}F_6$, and the cell parameters decrease monotonically with the decreasing of the Ln ionic radii, as shown in Table 1. Note that we present two values for the ionic radius (*r*),[21] corresponding to nine or six coordination numbers (CNs), both possible in these structures. By taking into account the Wyckoff positions and symmetries for all ions,[22] from refs 3 and 7, we used the site group method[23] to predict the irreducible representations of each site, and, then by their simple sum, we predicted the total reducible representations for each group. The results are presented in Tables 2 and 3, for the $P\bar{6}$ and $P6_3/m$ groups, respectively. We remark that each structure presents a site with two multiplicities that are half occupied by sodium ions, so we shall consider 10 atoms per primitive cell, leading to 30 degrees of freedom, distributed at the Brillouin zone center, as indicated. The predicted number and symmetries of the Raman and infrared-active modes are, then, summarized in these tables. We realize that,

(17) Grzechnik, A.; Bouvier, P.; Mezouar, M.; Mathews, M. D.; Tyagi, A. K.; Köhler, J. *J. Solid State Chem.* **2002**, *165*, 159.
(18) Rotereau, K.; Gesland, J.-Y.; Daniel, P.; Bulou, A. *Mater. Res. Bull.* **1993**, *28*, 813.
(19) Hayes, W.; Loudon, R. *Scattering of Light by Crystals*; John Wiley and Sons: New York, 1978.
(20) Porto, S. P. S.; Scott, J. F. *Phys. Rev.* **1967**, *157*, 716.
(21) Shannon, R. D. *Acta Crystallogr., Sect. A* **1976**, *32*, 751.
(22) Wyckoff, R. G. *Crystal Structures*; Wiley: New York, 1965.
(23) Rousseau, D. D. L.; Bauman, R. P.; Porto, S. P. S. *J. Raman Spectrosc.* **1981**, *10*, 253.

Table 2. Site Group Analysis for $NaLnF_4$ Crystals with the Burns $P\bar{6}$ Structure[a]

ion	Wyckoff site	site symmetry	irreducible representations
La^{3+}	1a	C_{3h}	$A'' + E'$
La^{3+}, Na^+	1f	C_{3h}	$A'' + E'$
Na^+, V_{Na}	2h	C_3	$A' + A'' + E' + E''$
F^-	3j	C_s	$2A' + A'' + 2E' + E''$
F^-	3k	C_s	$2A' + A'' + 2E' + E''$
total			$5A' + 5A'' + 7E' + 3E''$
Raman-active			$5A'(xx + yy, zz) + 6E'(xx^x - yy^x, xy^y, xx^y - yy^y, xy^x) + 3E''(xz, yz)$
infrared-active			$4A''(z) + 6E'(x, y)$

[a] The site positions and symmetries are from refs 3 and 13. The 2h site is half occupied (V_{Na} means Na vacancy).

Table 3. Site Group Analysis for $NaLnF_4$ Crystals with the $P6_3/m$ Structure[a]

ion	Wyckoff site	site symmetry	irreducible representations
Na^+, V_{Na}	2b	S_6	$A_u + B_u + E_{1u} + E_{2u}$
La^{3+}, Na^+	2c	C_{3h}	$A_u + B_g + E_{1u} + E_{2g}$
F^-	6h	C_s	$2A_g + A_u + B_g + 2B_u + E_{1g} + 2E_{1u} + 2E_{2g} + E_{2u}$
total			$2A_g + 3A_u + 2B_g + 3B_u + E_{1g} + 4E_{1u} + 3E_{2g} + 2E_{2u}$
Raman-active			$2A_g(xx + yy, zz) + E_{1g}(xz, yz) + 3E_{2g}(xx - yy, xy)$
infrared-active			$2A_u(z) + 3E_{1u}(x, y)$

[a] The site positions and symmetries are from ref 7. The 2b site is half occupied.

since $P\bar{6}$ is a piezoelectric group, some modes are respectively Raman- and infrared-active (see the 6E′ modes in Table 2). Conversely, $P6_3/m$ is a centro-symmetric group; therefore, for this structure, infrared (*ungerade*) and Raman (*gerade*) modes are mutually exclusive (Table 3). In the next sections, we will analyze the experimental results in terms of these predictions.

3.2. Infrared Reflectivity Spectra. The infrared reflectivity spectra of the $NaLnF_4$ single crystals recorded with the electrical field (E) parallel to the *x* and *z* axes are presented as solid circles in Figure 1a,b, respectively, in the spectral region 30−600 cm^{-1}. The bands are all relatively large and, for each configuration, the spectra for the different samples look very similar, which is a first indication that the crystals may be isostructural. We also point out the anisotropy between the spectra in both configurations.

The infrared spectra were obtained at quasi-normal incidence so that, for each polarization, the reflectivity $R(\omega)$ can be given by the Fresnel equation

$$R(\omega) = \left|\frac{\sqrt{\epsilon(\omega)} - 1}{\sqrt{\epsilon(\omega)} + 1}\right|^2 \quad (1)$$

where $\epsilon(\omega)$ is the complex dielectric function. In the infrared region, the dielectric function can be written in a factorized form in terms of the phonon contributions to the dielectric response, the so-called four-parameter semiquantum model, that is,[24]

$$\epsilon(\omega) = \epsilon_\infty \prod_{j=1}^{N} \frac{\Omega_{j,\mathrm{LO}}{}^2 - \omega^2 + i\omega\gamma_{j,\mathrm{LO}}}{\Omega_{j,\mathrm{TO}}{}^2 - \omega^2 + i\omega\gamma_{j,\mathrm{TO}}} \quad (2)$$

Table 4. Dispersion Parameters Calculated from the Fits of the Infrared Reflectance Spectra of $NaLaF_4$ Crystals by the Four-Parameter Semiquantum Model[a]

$NaLaF_4$	$\Omega_{j,\mathrm{TO}}$	$\gamma_{j,\mathrm{TO}}$	$\Omega_{j,\mathrm{LO}}$	$\gamma_{j,\mathrm{LO}}$	$\Delta\epsilon_j$
E ∥ *z*	55	18	64	34	6.683
	89	20	108	24	5.101
	143	19	159	32	2.280
	185	31	202	50	1.346
	242	28	297	49	2.523
	308	46	432	19	0.358
	$\epsilon_\infty{}^z = 2.453$			$\epsilon_0{}^z = 20.745$	
E ∥ *x*	227	13	243	42	4.380
	249	31	303	42	1.225
	307	33	328	41	0.105
	334	45	441	13	0.128
	$\epsilon_\infty{}^x = 2.413$			$\epsilon_0{}^x = 8.251$	

[a] The positions (Ω) and damping constants (γ) are given in cm^{-1}. The limiting values of the infrared dielectric constant are given, for each polarization.

In the expression above, ϵ_∞ accounts for the electronic contribution, $\Omega_{j,\mathrm{LO}}(\Omega_{j,\mathrm{TO}})$ and $\gamma_{j,LO}(\gamma_{j,\mathrm{TO}})$ are the frequencies and damping constants of the *j*th longitudinal (transverse) optical modes, respectively, and *N* represents the number of polar phonons.

The best fits of our experimental reflectivity data with the above equations are also presented in Figure 1a,b, as solid lines. These adjustments were made by using a nonlinear adjustment program developed by Meneses.[25] The complete set of phonon parameters obtained for the polar phonons is listed in Table 4, for the compound $NaLaF_4$. Note that we could discern six modes for E ∥ *z* and four modes for E ∥ *x*. The bands are all very broad, which is confirmed by the high values of the damping constants found in the fits. This table also presents the oscillator strength of the *j*th TO mode (for each polarization), $\Delta\epsilon_j$, and the limiting values of the dielectric constant at low and high infrared frequencies, ϵ_0 and ϵ_∞. Once the polar phonons have been determined, these constants are determined by

$$\Delta\epsilon_j = \frac{\epsilon_\infty}{\Omega_{j,\mathrm{TO}}{}^2} \frac{\prod_k (\Omega_{k,\mathrm{LO}}{}^2 - \Omega_{j,\mathrm{TO}}{}^2)}{\prod_{k\neq j} (\Omega_{k,\mathrm{TO}}{}^2 - \Omega_{j,\mathrm{TO}}{}^2)} \quad (3)$$

and

$$\epsilon_0 = \epsilon_\infty + \sum_{j=1}^{N} \Delta\epsilon_j \quad (4)$$

The ϵ_∞ values obtained for the electric field along the *x* or *z* axes are very close and present a good agreement with the refractive index value in the visible region ($n = 1.50$).[26] On the other hand, the ϵ_0 values present a high anisotropic character, also verified at radio frequencies,[10] whose origin is interesting to investigate. From Table 4, we can see that the two lowest frequency modes in the E ∥ *z* configuration

(24) Gervais, F.; Echegut, P. In *Incommensurate phases in dielectrics*; Blinc, R., Levanyuk, A. P., Eds.; North-Holland: Amsterdam, 1986; p 337.
(25) Meneses, D. D. *IRFit2.0 Adjustment Program*; Orléans University, France, 1999.
(26) Velsko, S. P.; Eimerl, D. *J. Appl. Phys.* **1987**, *62*, 2461.

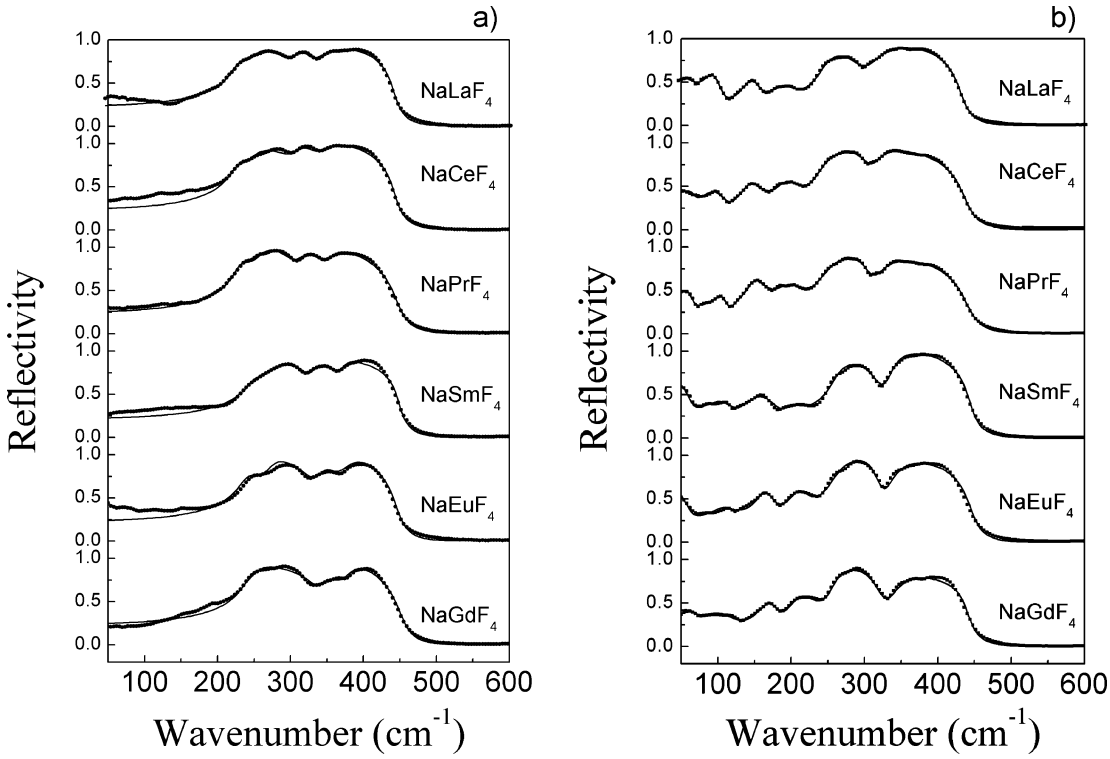

Figure 1. Infrared reflectivity spectra of $NaLnF_4$ single crystals recorded with the electrical field (a) perpendicular and (b) parallel to the principal axis (dotted curve). The solid lines represent the best fits to the four-parameter semiquantum model (see text).

Table 5. Assignment of the (Transverse/Longitudinal) Infrared-Active Modes of $NaLnF_4$ Crystals, for Increasing Ln Atomic Number[a]

assignment	$NaLaF_4$	$NaCeF_4$	$NaPrF_4$	$NaSmF_4$	$NaEuF_4$	$NaGdF_4$
A″ (TO/LO)	55/64	66/71	57/67	47/64	46/63	67/72
	89/108	98/114	107/113	106/121	111/120	109/131
	143/159	143/163	148/165	151/191	162/177	168/184
	185/202	190/208	193/213	197/200	206/221	207/239
	242/297	241/307	244/309	259/323	256/323	257/326
	308/432	312/438	316/442	333/444	332/447	336/441
$\epsilon_\infty^z/\epsilon_0^z$	2.45/20.7	2.45/18.7	2.45/18.0	2.45/26.9	2.53/22.1	2.53/18.5
E′ (TO/LO)	227/243	224/241	228/256	247/263	237/269	239/248
	249/303	246/307	257/311	269/325	270/340	249/340
	307/328	308/339	313/344	328/368	341/362	343/370
	334/441	342/443	348/448	369/449	370/447	374/452
$\epsilon_\infty^x/\epsilon_0^x$	2.41/8.25	2.38/8.71	2.45/9.07	2.49/7.68	2.45/8.25	2.53/8.65

[a] The wavenumbers, in cm^{-1}, were obtained from the maxima of the imaginary part of the dielectric constant and its reciprocal. The limiting dielectric constants are also given.

account for this anisotropy. However, for this configuration, we only expected four or two bands, with the predictions of $P\bar{6}$ (Table 2) and $P6_3/m$ (Table 3) groups, respectively. Then, if one of these groups were the correct one, the crystals present some extra modes (not predicted). Concerning the E || *x* configuration, we observed four bands, while, according to our predictions, we should have found six or three bands respectively for $P\bar{6}$ and $P6_3/m$ groups. In the next subsection, we demonstrate that these four bands are also seen in the Raman $z(xy)\bar{z}$ spectrum of this crystal, which indicates that the correct structure would be $P\bar{6}$. Since the spectra of the different Ln samples look similar, we will assign the observed phonon modes of all crystals to the irreducible representations of this group. The Raman results that will be presented in the sequence confirm this choice. The origin of the extra modes for E || *z* will be discussed later.

We present now, in Table 5, a summary of the main optical parameters used to fit the experimental data for the other $NaLnF_4$ crystals, that is, the frequencies of the TO/LO modes and the limiting values of the dielectric constants. We note first that the same set of modes was observed for all crystals and that, except for the lowest frequency E || *z* mode (A″ type), all modes shift to higher frequencies with decreasing ionic radii. Physically, the first observation indicates that the crystals should be isostructural. In this case, the second one can be simply explained as the enhancement of the ionic interactions because of the atomic volume decrease, an effect similar to the hardening of the vibrations by volume contraction upon cooling a sample. The anomalous behavior of the cited band seems to indicate that this mode is less sensitive to volume changes. However, we must consider the lowest precision in the determination of the positions of the maxima of TO and LO modes, because the bands are very large. The two lowest frequency E || *z* modes are responsible for the higher static dielectric constant in this configuration and for the large variation in this parameter

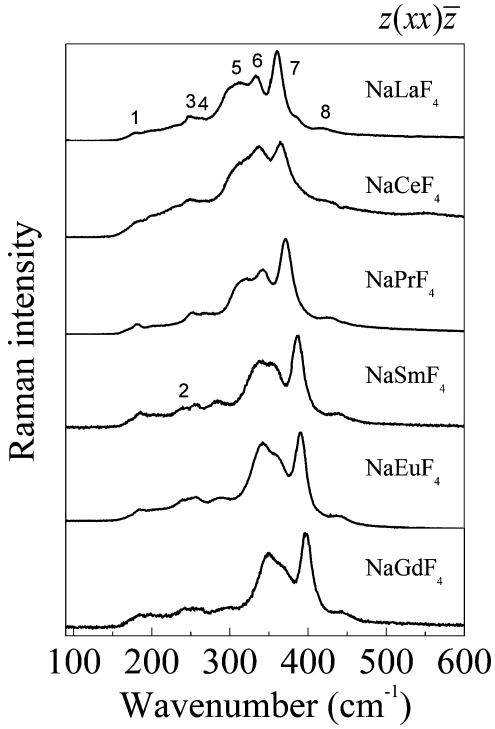

Figure 2. Polarized backscattering Raman spectra of $NaLnF_4$ single crystals for the $z(xx)\bar{z}$ scattering geometry.

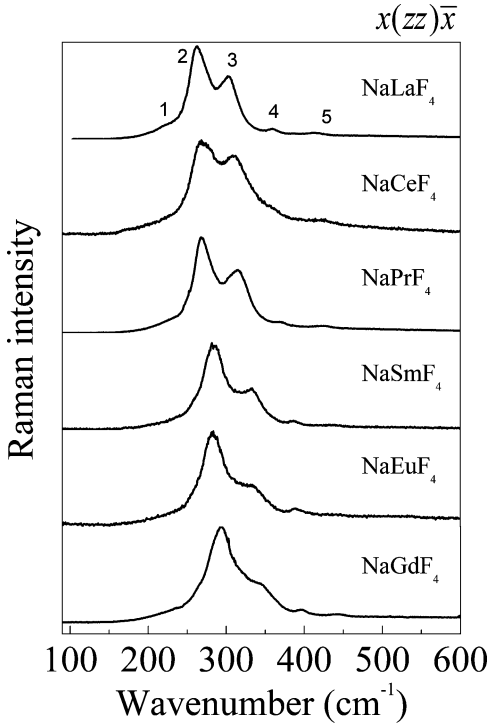

Figure 3. Polarized backscattering Raman spectra of $NaLnF_4$ single crystals for the $x(zz)\bar{x}$ scattering geometry.

for different Ln ions. As we will later discuss, that these two modes may be those we called extra modes, that is, modes that were not predicted by group theory.

3.3. Raman Scattering. The Raman spectra of $NaLnF_4$ crystals in the $z(xx)\bar{z}$ scattering geometry are presented in Figure 2, for increasing Ln atomic number, from top to bottom. The spectra for the six different samples look very similar, being constituted of rather broad bands. By using Lorentzian lines we can depict, by fitting, up to eight bands. According to group theory predictions for the $P\bar{6}$ group, one should have 11 bands in this configuration, that is, $5A' + 6E'_{TO}$ (see Table 2), while for the gagarinite group only five bands of $2A_g + 3E_{2g}$ types were predicted (Table 3).

The totally symmetric modes can be obtained separately by using the $x(zz)\bar{x}$ scattering geometry. The result for our crystals is presented in Figure 3, in the same atomic number sequence. We can discern up to five bands for most crystals. However, two of these bands are very strong, whereas the other three are rather faint. Therefore, we preferred to use the degenerate modes which appear in $z(xx)\bar{z}$ geometry to check the structure. These modes can be observed separately by using a $z(xy)\bar{z}$ configuration. The spectra obtained for our samples in this configuration are presented in Figure 4. The similarity of the spectra for different Ln samples is still clearer. We can discern six bands in each spectrum, with perfect agreement with group theory predictions for the Burns $P\bar{6}$ structure. Before comparing the positions of these bands with those obtained by infrared spectroscopy, we will present the Raman spectra for the $y(xz)\bar{y}$ geometry, where one expects to observe the other doubly degenerate modes. These spectra are shown in Figure 5. In this case, we can discern four Lorentzian lines, exceeding the predicted number of modes (three 3E″ modes for the *Burns* structure, one E_{1g} for the gagarinite one).

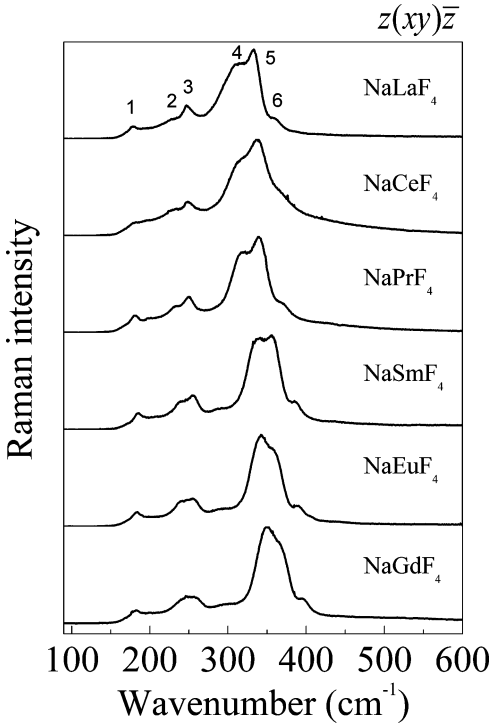

Figure 4. Polarized backscattering Raman spectra of $NaLnF_4$ single crystals for the $z(xy)\bar{z}$ scattering geometry.

The fitting parameters for the Raman bands of our six crystals, in the four used scattering geometries, are presented in Table 6, together with the modes assignment to the Burns structure. At this point, we can compare the frequencies of the $6E'_{TO}$ Raman modes with the corresponding values obtained by infrared spectroscopy with E || *x*, where only four bands were discerned. The agreement between these spectra is remarkable and constitutes a proof of the correctness of the Burns structure. The two missing modes in the

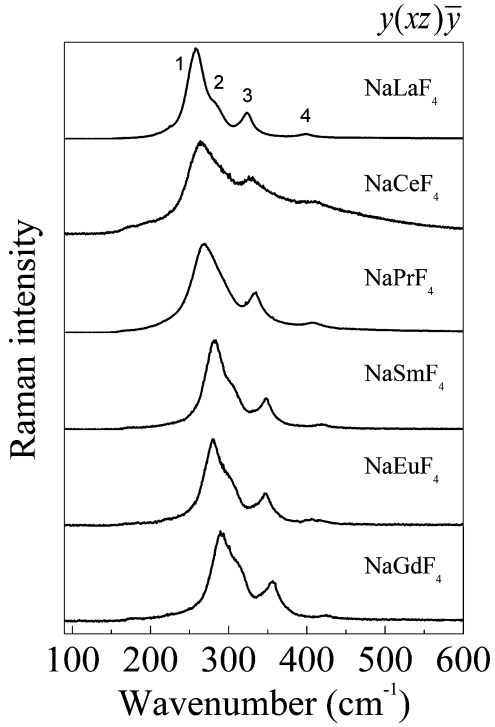

Figure 5. Polarized backscattering Raman spectra of $NaLnF_4$ single crystals for the $y(xz)\bar{y}$ scattering geometry.

infrared spectra are those that appeared at higher and lower frequencies in the Raman spectra. The fact that they are absent in the infrared spectra means that the dipole moments associated with these movements are too weak.

Hence, we remark that from the 15 bands showed in Table 6 (for each crystal), 13 present an important shift to higher frequencies for increasing Ln atomic number, while one E'_{TO} mode (no. 1) presents only a relatively lower upshifting and another E'_{TO} mode (no. 3) does not change its position. In the first case, the Raman spectra evolution with different Ln ion is the same as that observed in the infrared spectra and was attributed to the unit cell volume contraction for smaller Ln ions (Table 1). The two Raman bands that do not follow that trend may depend on the mass of Ln ions, with lower influence of the unit cell volume. Unfortunately, we could not prepare $NaYF_4$ single crystals to check this conjecture.

The Raman and infrared results presented above show undoubtedly that the $NaLnF_4$ crystals for Ln = La−Gd are isostructural and belong to the Burns $P\bar{6}$ structure. Besides solving the controversy on the structure of the La-, Ce-, and Pr-based crystals,[11,13,16] this result is interesting because Burns[13] and Fedorov[16] agreed that $NaSmF_4$ should belong to the gagarinite structure, in conflict with our findings. Although we did measure neither Ln-based crystal with lower ionic radii nor $NaYF_4$, we believe that $P\bar{6}$ could also be the correct structure for all these crystals. It is worthy to mention that $NaLaF_4$ presents second harmonic generation[26] and piezoelectricity,[10] two macroscopic properties that are compatible with this group. We also verified piezoelectric activity for all the $NaLnF_4$ crystals studied here, denying the existence of an inversion center in the structure.

The group theory predictions for the normal modes of $NaLnF_4$ at the Brillouin zone center, for the $P\bar{6}$ structure, lead to 18 modes, distributed in their irreducible representations as $5A' + 4A'' + 6E' + 3E''$. For our crystals, we could assign the 5A′ and the 6E′ modes. Nevertheless, we observed six A″-type and four E″-like modes, that is, two and one extra modes, respectively, for these symmetries. These modes can be originated from defects in the crystal structure. Indeed, the very broad vibrational bands indicated that disorder is important in these crystals. One kind of disorder comes from the random occupancy of 1f Wyckoff sites by Ln^{3+} and Na^+ ions that share equally this site.[5,26] Some ordering could occur, decreasing the local symmetry (which is averaged over the ions). The other kinds are linked to the 2h site. While 1a and 1f sites are nine-fold coordinated, 2h site is orthogonally coordinated (CN = 6) and presents 50% of occupancy by Na^+.[17] There are, then, two possible defects in this site: one is the local breaking of symmetry, by partial ordering of Na^+ ion (producing locally a polarlike structure); the other is the

Table 6. Assignment of the Observed Raman-Active Modes of $NaLnF_4$ Crystals, for Increasing Ln Atomic Number[a]

geometry	no.	$NaLaF_4$	$NaCeF_4$	$NaPrF_4$	$NaSmF_4$	$NaEuF_4$	$NaGdF_4$	modes
$z(xx)\bar{z}$	1	178/18	179/20	181/22	185/18	187/32	185/53	E'_{TO}
	2				239/22	238/9	244/39	E'_{TO}
	3	247/11	248/19	251/12	256/11	255/37	253/45	E'_{TO}
	4	264/39	270/35	271/35	284/19	286/29	293/28	A′
	5	312/36	311/32	314/43	335/38	340/37	348/37	E'_{TO}
	6	334/17	337/33	343/20	358/20	363/26	370/21	E'_{TO}
	7	361/17	366/24	372/17	386/20	391/17	398/17	A′, E'_{TO}
	8	421/22	429/23	433/16	440/23	442/25	445/26	A′
$x(zz)\bar{x}$	1	218/34	198/17	221/15	229/28	222/39	229/34	A′
	2	264/29	269/36	269/30	284/35	284/30	292/40	A′
	3	303/33	312/59	315/44	332/40	332/41	342/66	A′
	4	360/15	365/25	365/16	384/23	390/10	397/17	A′
	5	424/28	425/30	424/32	438/35		453/27	A′
$z(xy)\bar{z}$	1	179/16	183/38	180/14	185/13	184/17	184/19	E'_{TO}
	2	227/10	230/18	232/18	238/17	240/14	244/20	E'_{TO}
	3	248/14	249/13	250/19	252/29	251/18	250/20	E'_{TO}
	4	311/49	313/40	316/34	336/37	340/30	348/29	E'_{TO}
	5	334/18	339/31	341/24	358/22	362/22	368/25	E'_{TO}
	6	358/18	370/35	374/22	386/16	387/17	394/15	E'_{TO}
$y(xz)\bar{y}$	1	258/25	261/24	266/25	281/24	279/24	289/25	E″
	2	284/16	281/36	285/37	303/25	301/26	311/28	E″
	3	322/22	329/34	335/21	347/20	347/21	356/22	E″
	4	399/17	412/17	409/21	420/16	408/16	425/12	E″

[a] The wavenumbers and line widths, obtained from Lorentzian fits, are in cm^{-1}.

occupation of this site by the Ln^{3+} ions, which is possible because their ionic radii are all compatible with the available space (except for La^{3+}, they are smaller than the sodium ion), as shown in Table 1. The last type of defects has been experimentally verified,[3,4] being considered responsible for the high luminescence efficiency of this system.[5,17] The presence of such defects could add up to four modes to the optical vibrational spectrum, decomposed in the irreducible representation of the crystal group symmetry as $A' + A'' + E' + E''$. This would happen in the condition in which the crystal field was strong enough to distinguish the off-site cations.[27] Some of the additional bands could be relatively weak, which is not in contradiction with our results (remember we found one Raman E″ extra mode, and two polar A″ extra modes). It is interesting to note that the A″ modes are polarized along the *z* axis and that a breaking of symmetry in 2h sites would lead to a polarization in this direction (see the structure in ref 17). Then, we consider that the two types of disorder in the half-occupied 2h site are responsible for the main anomalous effects observed here: broad vibrational bands, presence of extra modes, and high dielectric constant along the *z* direction. However, thanks to these defects, $NaLnF_4$ crystals can be appointed as promising laser host matrixes.

(27) Moreira, R. L.; Matinaga, F. M.; Dias, A. *Appl. Phys. Lett*. **2001**, *78*, 428.

4. Conclusions

Large optical quality $NaLnF_4$ crystals have been grown by the Czochralski technique, for Ln = La, Ce, Pr, Sm, Eu, and Gd. The crystals were investigated by polarized Raman scattering and infrared reflectance spectroscopy. The optical phonon spectra show that all materials are isostructural. Moreover, they obey well the selection rules for the hexagonal $P\bar{6}$ structure, where the chemical formula is written as $Na_{1.5}Ln_{1.5}F_6$, with one formula per unit cell. The complete set of optical vibrational modes at the Brillouin zone center was determined for each crystal and is assigned to their respective irreducible representations. The presence of three extra bands was attributed to cationic disorder, mainly in the half-occupied 2h site. This disorder is also responsible for the broadening of all bands and should play an important role in the luminescence efficiency of the materials.

Acknowledgment. The authors are grateful to CNPq, CAPES, and Fapemig (Brazil) and CNRS (France) for partially funding this work and to A. M. Moreira for his help in the Laue experiments.

CM050860K